Characteristics of Superficially-Porous Silica Particles for Fast HPLC: Some Performance Comparisons with Sub-2-µm Particles

J.J. DeStefano*, T.J. Langlois, and **J.J. Kirkland**
Advanced Materials Technology, Inc., 3521 Silverside Rd., Suite 1-K, Quillen Bldg., Wilmington, DE 19810

Abstract

Columns of 2.7-µm fused-core (superficially porous) Type B silica particles allow very fast separations of small molecules at pressures available in most high-performance liquid chromatography instruments. These highly-purified particles with 1.7-µm solid silica cores and 0.5-µm-thick shells of 9 nm pores exhibit efficiencies that rival those of totally porous sub-2-µm particles but at one-half to one-third of the column back pressure. This presentation describes other operating features of fused-core particle columns, including sample loading characteristics and packed bed stability. The superior mass transfer (kinetic) properties of the fused-core particles result in much-improved separation efficiency at higher mobile phase velocities, especially for > 600 molecular weight solutes.

Background

There has been strong recent interest in techniques and apparatus for performing very fast high-performance liquid chromatography (HPLC) separations. The reasons for this are quite understandable. Rapid and reliable analyses facilitate research studies leading to new products, solve important environmental problems, and produce new and better ways to attack health problems. It has been known for some time that high-speed separations without loss in separating power can be achieved by reducing the size of particles in columns (1). However, while a two-fold reduction in particle size can lead to a 1.4-times (square root of 2) increase in column efficiency, the pressure drops within columns of equal dimensions increases fourfold. This situation then forces a compromise between particle size, column length, and pressure that have been the subject of many studies (2,3).

Some workers find that columns with 3- or 3.5-µm particles operated at a rather high flow rate are able to solve their fast-analysis problems using modest operating pressures. For even faster separations, columns with even smaller, so-called sub-2-µm particles have recently been commercialized (4–6). However, these totally porous sub-2-µm particle columns create some practical problems for users that must be overcome. HPLC instruments with 400 bar pressure limits often do not produce flow rates for some columns that result in optimum column efficiency because the plate height minimum is not reached with available mobile phase velocities (6). To overcome this limitation, manufacturers now have made available instruments capable of higher operating pressure, up to 1000 bar, and these provide the capability to operate sub-2-µm columns at higher flow rates and higher efficiencies. These new sophisticated instruments do not, however, eliminate some of the other experimental deficiencies, such as the need to filter samples and mobile phases to minimize pluggage of the 0.5-µm frits that must be used with sub-2-µm particle columns. In addition, columns of present sub-2-µm particles still do not produce the efficiency expected for the particle size, and some of the columns experience a degradation of performance with use, especially at high pressures (discussed later).

As one effective answer to the compromise between efficiency, analysis speed, and operating pressure, new fused-core particles have been developed that allow highly efficient, very fast separations with modest operating pressures. These highly purified 2.7-µm superficially porous silica particles have a solid core and a 0.5-µm-thick shell with 9 nm pores. Packed columns of these fused-core particles show efficiencies not previously reported for totally porous particles of equivalent size. In addition, the thin porous shell exhibits excellent mass transfer (kinetic) of solutes. This property allows solute molecules to rapidly enter and exit the porous structure for interaction with the stationary phase. As a result, high mobile phase velocities can be used for very fast separations with only modest loss in column efficiency. A previous publication has briefly described some of the properties of the fused-core particles and their uses (7). This experimental presentation more fully describes the characteristics of the fused-core particles and compares packed-column performance with that of conventional totally porous particles. Other recent publications have

* Author to whom correspondence should be addressed: email joedestefano@advanced-materials-tech.com.

described some of the largely theoretical aspects of fused-core particles (8–11) and the use of columns of these materials in HPLC–mass spectrometer applications (12).

Experimental

Fused-core particles and Halo columns were from Advanced Materials Technology, Inc. (Wilmington, DE). The 2.7-µm high-purity Type B silica particles have a 1.7-µm solid silica core and a 0.5-µm-thick porous shell with 9 nm pores. Figure 1 is a cross-section electron photomicrograph of these particles as supplied by Micron, Inc. (Wilmington, DE). Figure 2 gives mercury intrusion and exclusion of these particles (Micromeretics Analytical Services, Norcross, GA), illustrating the pore size and some characteristics of the pores. The similar intrusion/exclusion plots suggest the good strength of the porous shell and a minimum of "ink bottle" pores in the structure. The nitrogen surface area of the unmodified fused-core particles is 150 m^2/g as measured on a Micromeritics Gemini V surface area and pore size analyzer (Norcross, GA). Particle sizes and distributions were measured with a Multisizer 3 Coulter Counter (Beckman Coulter, Fullerton, CA). A densely bonded and endcapped monofunctional dimethyl-C18 stationary phase was prepared on the fused-core particles by a conventional reaction (13) with silanes obtained from Gelest, Inc. (Morrisville, PA).

Chromatographic data were obtained on a model 1100 instrument (Agilent Technologies, Palo Alto, CA) using UV detection with a 2-µL detector cell. Data were recorded from the model 1100 ChemStation (Agilent). All connectors to the column and detector were 0.005-in i.d. tubing to minimize extra-column effects. Data were acquired with a detector response time of 0.1 s. In addition, a data sampling rate of at least 20 points/s was used so that a minimum of 20 points/s would be obtained on the very sharp, low volume peaks obtained on the fused-core Halo columns. Stainless steel column hardware and column frits with 2-µm porosity were obtained from Isolation Technologies (Hopedale, MA). Columns used in this study were prepared by slurry-packing techniques using in-house-designed hardware (14). Chromatographic tests were performed using injections from a model 8125 sampling valve (Rheodyne, Cotati, CA).

Plate heights were calculated by the peak half-height/width method (15). Data for the reduced plate height versus mobile phase velocity plots were fitted to the Knox equation:

$$h = Au^{1/3} + B/u + Cu \qquad \text{Eq. 1}$$

where h is the reduced plate height (plate height H/particle

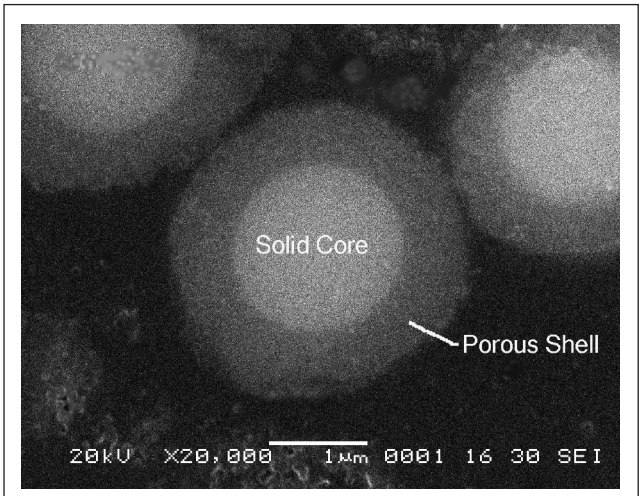

Figure 1. Electron micrograph cross-section of a fused-core particle with 9 nm pores.

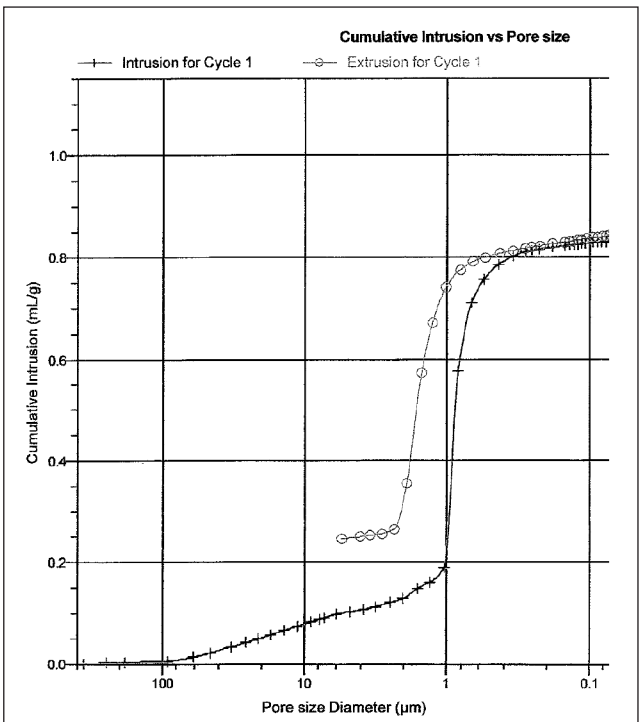

Figure 2. Mercury intrusion/exclusion of fused-core particles with 9 nm pores.

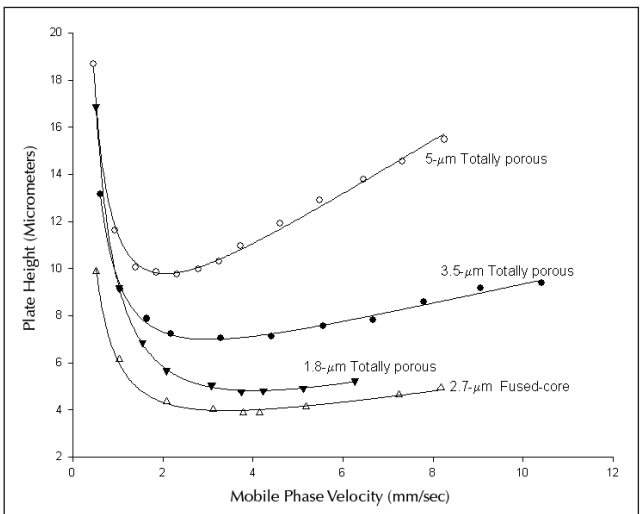

Figure 3. Effect of particle type. Columns: 50 × 4.6 mm; solute: naphthalene; mobile phase: 60% acetonitrile–40% water; temperature 23°C.

diameter, d_p); A, B, and C are column coefficients; and u is the mobile phase velocity (15). Solvents for mobile phases were from Mallinckrodt Baker (Philipsburg, NJ) and used as received. Test solutes were from Sigma-Aldrich (St. Louis, MO) and used as received.

Results and Discussion

The unusually high efficiency of fused-core columns is illustrated in Figure 3. As expected from theory, the plate heights for 50 × 4.6 mm i.d. columns are increasingly smaller as particle size decreases from 5- to 1.8-µm. Unexpectedly however, the plate height for the 2.7-µm fused-core column is lower than that for a column of smaller 1.8-µm totally porous particles. The experimental data of Figure 4 shows the reduced plate height (plate height H divided by particle diameter, d_p) plots for columns of smaller totally porous particles and a column of fused-core particles. The 3- and 3.5-µm particles produce reduced plate height minima of approximately two for small molecules. This value has been traditionally considered as the "limit" for excellent columns of totally porous particles. On the other hand, the column of fused-core particles has a plate height minimum of approximately 1.5, which is consistently seen for columns of these particles. In fact, longer columns (e.g., 150 mm) of these particles show reduced plate heights as small as 1.2 because of reduced extra-column band broadening effects of the larger-volume column (not shown here). Figure 4 also shows the pressure required for the highest mobile phase velocity attempted for each column in this study. As expected, the larger particles show lower pressure drops, and the smaller particles higher pressure drops, with the column of 1.8-µm particles showing the highest pressure requirements at much smaller mobile phase velocities.

The larger reduced plate heights of the 1.8-µm particles in

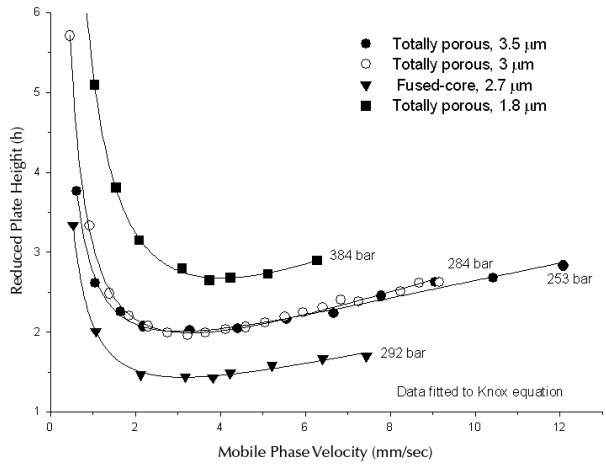

Figure 4. Van Deemter plots of totally porous and fused-core particles. Columns: 50 × 4.6 mm; mobile phase: 60% acetonitrile–40% water; bonded phase: C18; solute: naphthalene; temperature: 24°C.

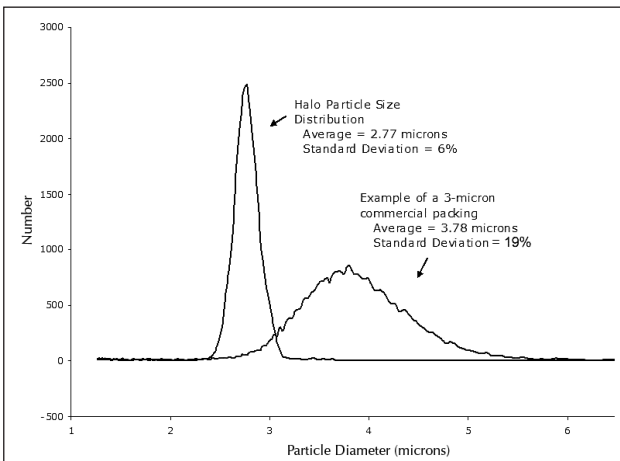

Figure 5. Particle size distribution of 2.7-µm fused-core and 3-µm totally porous particles.

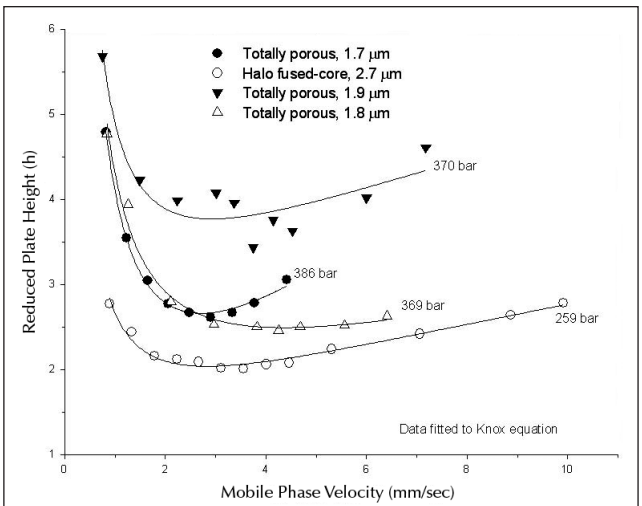

Figure 6. Reduced plate height plots for columns of sub-2-µm and fused-core particles. Columns: 50 × 2.1 mm, C18; mobile phase: 70% acetonitrile–30% water; temperature: 24°C and solute: acenaphthene.

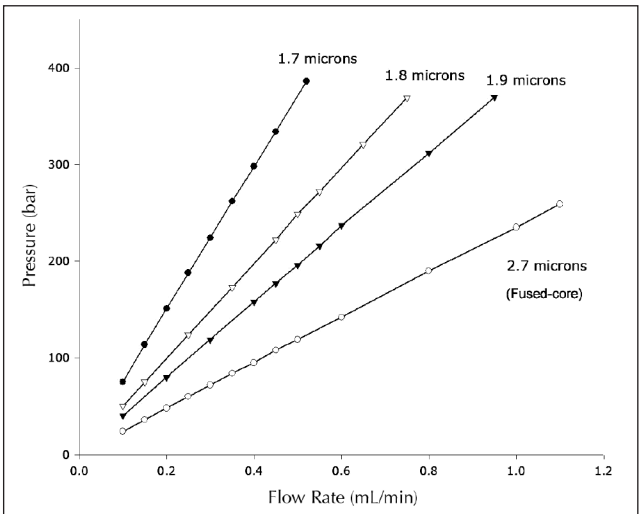

Figure 7. Column pressure plots for columns of sub-2-µm and 2.7-µm fused-core particles. Conditions as in Figure 6.

Figure 4 suggest that there is difficulty in obtaining homogeneous packed beds of these very small particles. On the other hand, the unusual efficiency of the column of fused-core particles may be explained by the very narrow particle size distribution of this material, as shown in Figure 5. The standard deviation of the fused-core particle size distribution typically is 5–6%, while the standard deviation of high-quality 3-µm totally porous particles in Figure 5 is approximately 19%. The very narrow size particle distribution of the fused-core particles, coupled with the higher density of this material (30–70% more dense compared to totally porous particles, depending on porosity), apparently allows the formation of very homogeneous packed beds. Computer simulations (16) and other studies (17) have both suggested that narrower particle size distributions result in more homogeneous packed beds of higher efficiency. Therefore, very narrow particle size distributions appear to be preferred for better packed beds with higher efficiency and stability. We speculate that the resulting excellent packed-bed homogeneity probably leads to the unusual efficiency of the fused-core particle columns (i.e., smaller A-term of Equation 1).

Figure 6 compares the reduced plate height plots for 50 × 2.1 mm columns of fused-core particles and several commercial sub-2-µm particles. In all cases, columns of the sub-2-µm particles show significantly higher reduced plate values, suggesting poorer packed bed homogeneity compared to the fused-core particle column. The packed bed of the 1.9 µm particles was so unstable that it was difficult to accurately measure data for some of the mobile phase velocity points. The highest mobile phase velocity for each column resulted in column pressures less than 400 bar. Plate heights H of these 2.1 mm i.d. columns is approximately 20% less than those for 4.6 mm id columns, largely because of extra-column band broadening effects of the smaller diameter (and lower volume) columns producing very sharp, low-volume peaks. Nevertheless, the fused-core column shows only approximately 20% lower plates from the best sub-2-µm columns even though the particle size is much larger.

However, as a result of the larger particle size, fused-core particles operate at much lower back pressures than sub-2-µm particles, as illustrated in Figure 7. At the same flow rate, fused-core particles require one-half to one-third the pressure as for sub-2-µm particle columns. This feature results in the ability to operate at higher flow rates (and faster separations) with conventional HPLC hardware limited to pressures such as 400 bars.

A further comparison of fused-core particle columns with sub-2-µm particle columns is shown in Figure 8. This figure compares plate number, pressure (bar), and plates/pressure (bar) for the same columns of Figure 6, all data taken at the plate height minimum. Here, the advantage of the fused-core particles in terms of available plates as a function of pressure requirements is clearly shown. This result is especially useful

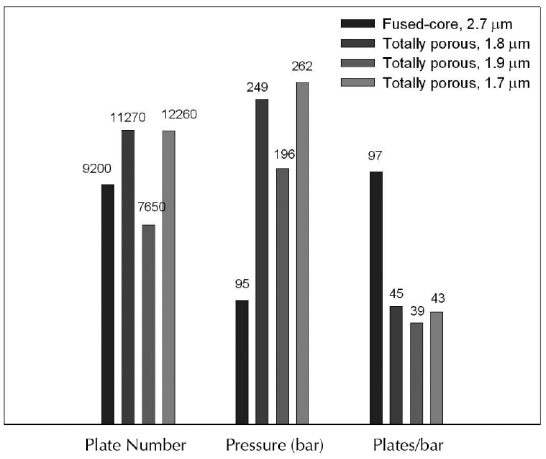

Figure 8. Plates/pressure comparison for columns of sub-2-µm and 2.7-µm fused-core particles. Conditions as in Figure 6.

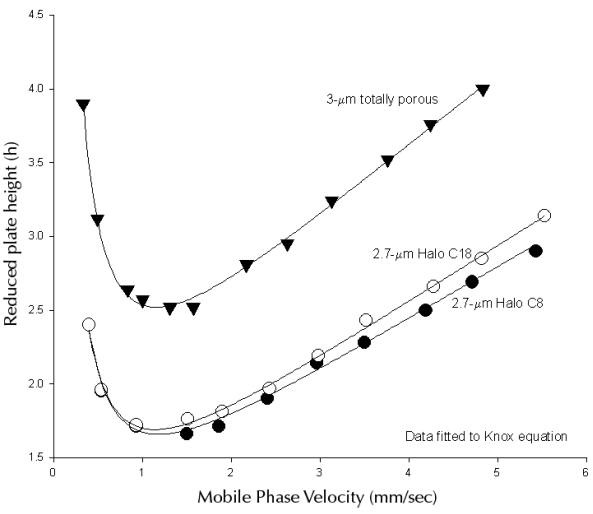

Figure 9. Reduced plate height plots for virginiamycin. Columns: 50 × 4.6 mm, C18, C8; particles: 3-µm totally porous, 2.7-µm fused core; mobile phase 35% acetonitrile–65% potassium phosphate buffer, pH 3.0; temperature: 30°C. *(Data courtesy of W. Campbell, Supelco, Inc.).*

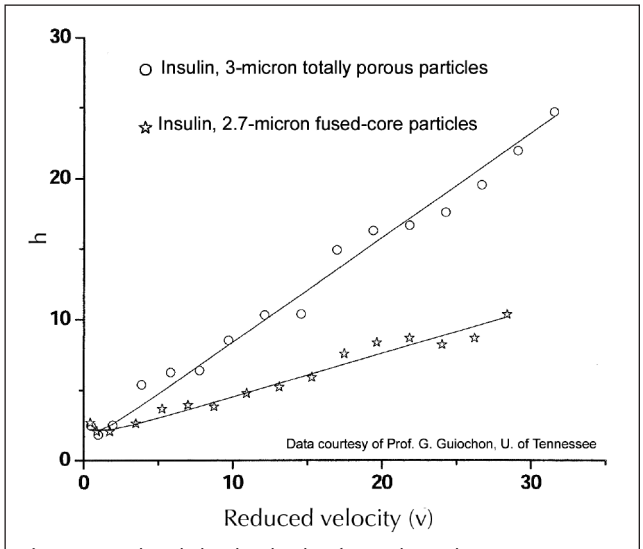

Figure 10. Reduced plate height plots for insulin. Columns: 50 × 4.6 mm C18; particles: 3-µm totally porous and 2.7-µm fused-core; mobile phase: acetonitrile–water–trifluoroacetic acid 32:60:0.1% (v/v); temperature: 60°C. *(Data courtesy of Prof. G. Guiochon, Univ. Of Tennessee [18]).*

in situations where very high operating pressures are not available on instruments. For example, instruments with a 400 bar pressure limitation can still be used for operating columns of fused-core particles at high mobile phase velocities for very fast separations.

Compared with totally porous particles, the thin porous shell on fused-core particles results in improved mass transfer (kinetic) effects where solutes diffuse more quickly in and out of the porous structure for interaction with the stationary phase. For smaller molecules (e.g., MW < 600) this effect is not so dramatic, as shown in Figure 9. Here, columns of fused-core particles with C18 and C8 stationary phases show improved reduced plate heights over a 3-µm totally porous particle column for virginiamycin (MW = 574) at the reduced plate height minimum. This effect (smaller A-term of Equation 1) is mainly due to the homogeneous packed bed for the fused-core particles. Note also that the slope of the plot with the fused-core column is slightly less steep than for the totally porous particle column. This lower slope of the plot suggests that the C-term of Equation 1 is somewhat smaller for this larger solute, indicating that improved mass transfer effects are beginning to take place because of shorter diffusion paths in the porous shells.

For the present fused-core particles, C-term improvement begins to be obvious at approximately 600 molecular weights and is significant for molecules with approximately 1000 molecular weights. For still larger solutes, the improved mass transfer of the fused-core particles becomes impressive at higher mobile phase velocities, as shown in Figure 10 for insulin. At higher reduced velocities, the fused-core particle column exhibits reduced plate heights almost half that of totally porous particles of approximately the same size. Under these operating conditions, the tight molecular conformation of this ionizable solute allows insulin (5800 Dalton) to largely access the 9 nm pores of the fused-core particles. This improved mass transfer characteristic of the fused-core particles is especially attractive for carrying out very fast separations of larger compounds that can access the porous structure.

Relative to totally porous particles of higher nitrogen surface area, fused-core particles maintain satisfactory sample loading characteristics for conducting demanding analyses, as shown in Figure 11. The data for 150 × 4.6 mm columns show closely similar sample loadability for 150 m^2/g fused-core particles and 440 m^2/g totally porous particles as indicated by the peak symmetry for phenol and diphenhydramine at low pH as the concentration is increased. Such results confirm the capability of fused-core particle columns to operate in situations where measurements of both major and minor components are required in the same separation.

Rigorous tests have confirmed the data in the literature (7) regarding the unusual stability of fused-core particle packed beds. Figure 12 shows the overlaid first and 500th chromatograms of a pharmaceutical sample separated on a 100 × 4.6 mm C18 fused-core particle column at 35°C, 2.0 mL/min, and a column pressure of 260 bar. Also shown in the figure are the standard deviations found for variation in retention times, plates, peak tailing, and resolution for peaks C and D during the study. An even more stringent fused-core column stability test is shown in Figure 13. The figure shows overlaid

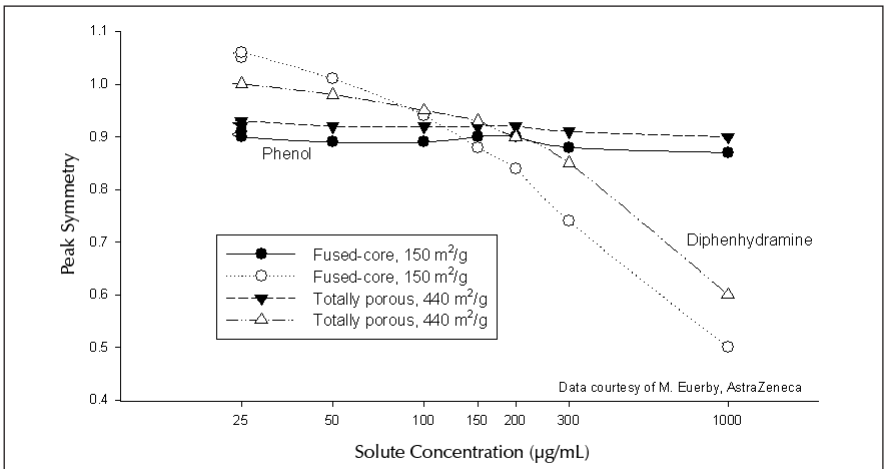

Figure 11. Sample loading study. Columns: 150 × 4.6 mm, Halo C18; particles: 3-µm totally porous (440 m^2/g), 2.7-µm fused-core, 150 m^2/g; mobile phase: A = 20 mM KH_2PO_4 pH 2.7; B = 20 mM KH_2PO_4, pH 2.7 in 35:65 (v/v) water–methanol; A:B = 30:70 (v/v); detection: 214 nm; temperature: 60°C; injection: 5 µL. *(Data courtesy of Dr. Mel Eureby, AstraZeneca).*

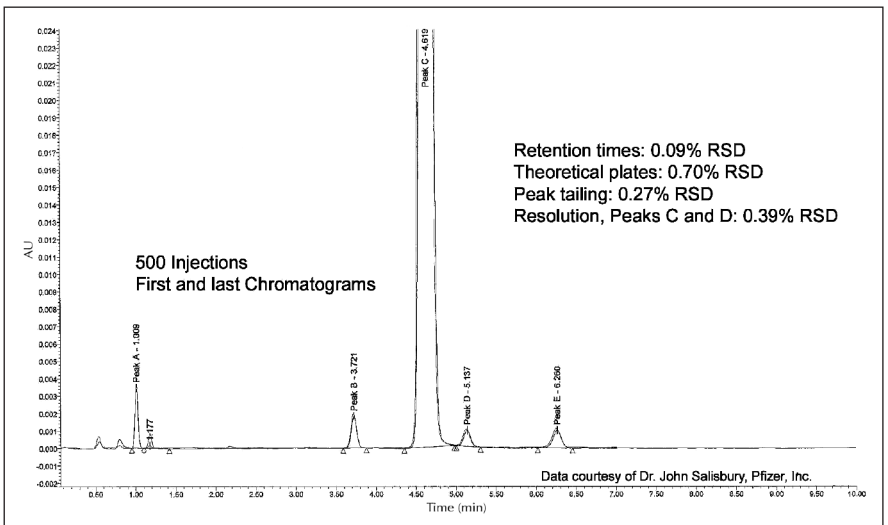

Figure 12. Column stability test after 500 injections. Column: 100 × 4.6 mm fused-core C18; mobile phase: 70% acetonitrile–30% water; flow rate: 2.0 mL/min; temperature: 35°C; pressure: 260 bar. *(Data courtesy of Dr. John Salisbury, Pfizer, Inc.).*

chromatograms for the first and 250th injection of another pharmaceutical sample carried out on a 100 × 2.1 mm C18 fused-core particle column at 30°C, 1.6 mL/min, and a column pressure of 835 bar. Also shown on the figure are the standard deviations found for variations of retention, plates, peak tailing and resolution of peak 1 and 2 during the column stability study. These data illustrate the excellent stability of fused-core particle packed beds, even under column pressures well above the 400 bar operating limits of many HPLC instruments. This unusual column stability is attributed to the ability to pack extremely homogeneous beds as a result of the very narrow particle size distribution of the fused-core particles.

The capability of a fused-core column to carry out very fast separations of mixtures is illustrated in Figure 14. This mixture of eight herbicides can be separated in approximately 40 s under isocratic conditions. An interesting, often unrecognized additional advantage of fused-core particle columns is that, because of the solid core and the smaller porous volume of the thin outer shell, unretained solutes (t_0) are more quickly eluted than for totally porous particles of the same size. This further increases separation speed by reducing the "dead" time of the column, approximately one-half that for comparable columns of totally porous particles.

Gradient separations also can be performed rapidly as shown in Figure 15. This mixture of fourteen explosives is separated in 3 min using conditions that are readily available in most instruments.

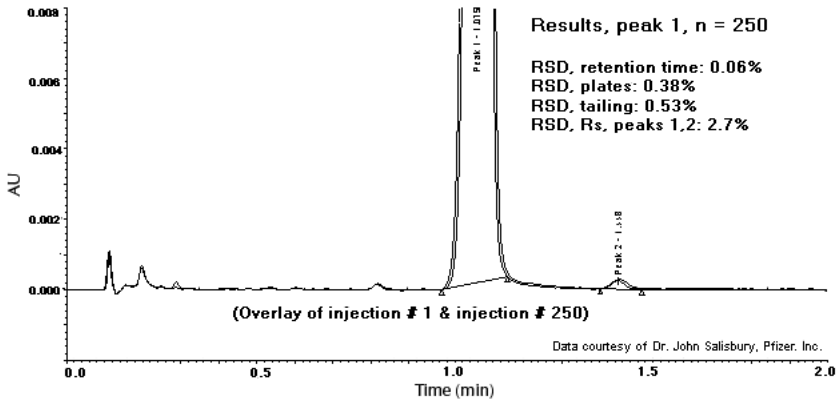

Figure 13. Column stability study at 835 bar. Column: 100 × 2.1 mm C18 fused-core particles; mobile phase: 70% acetonitrile–30% water; flow rate: 1.6 mL/min; temperature: 30°C; column pressure 12264 psi (835 bar); number of injections: 250. *(Data courtesy of Dr. John Salisbury, Pfizer, Inc.).*

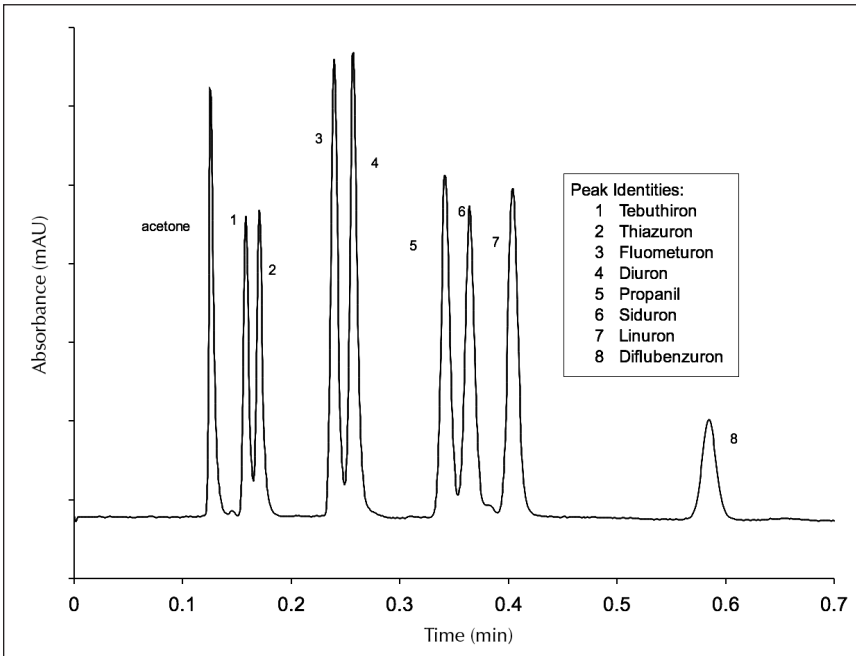

Figure 14. Fast (40 s) isocratic separation of pesticides. Column: 50 × 4.6 mm C18 fused-core particles; mobile phase: 45% acetonitrile–55% water; flow rate: 4.0 mL/min; temperature: 60°C; pressure: 230 bar; detection: UV at 245 nm.

Conclusions

Columns of new silica 2.7-µm fused-core particles with solid cores and a 0.5-µm-thick porous shell of 9 nm exhibit unusual chromatographic efficiency, with reduced theoretical plates of 1.5 or lower for small molecules. Presumably, this is due to the ability to form very homogeneous packed beds as a result of an extremely narrow particle size distribution and higher particle density. These columns with homogeneous packed beds are also highly stable at operating pressures of at least 600 bar. Sample loading characteristics of fused-core columns for practical separations closely resemble those of the totally porous particles with higher surface areas. Fused-core particles exhibit highly improved mass transfer (kinetic) effects because of the thin porous shell surrounding a solid core, allowing solutes to rapidly diffuse in and out of the porous structure containing the stationary phase for interaction. Compared to totally porous particles, the fused-core configuration significantly improves column efficiency at high mobile phase velocities for compounds above approximately 600 molecular weights. For solutes above approximately 2000 molecular weight, column efficiency can approximately double, compared to columns of totally porous particles. Columns of the fused-core particles exhibit theoretical plates nearly comparable to those of sub-2-µm particles, but with much reduced pressure requirements. Stated otherwise, the fused-core particles generally develop appproximately twice the theoretical plates/bar

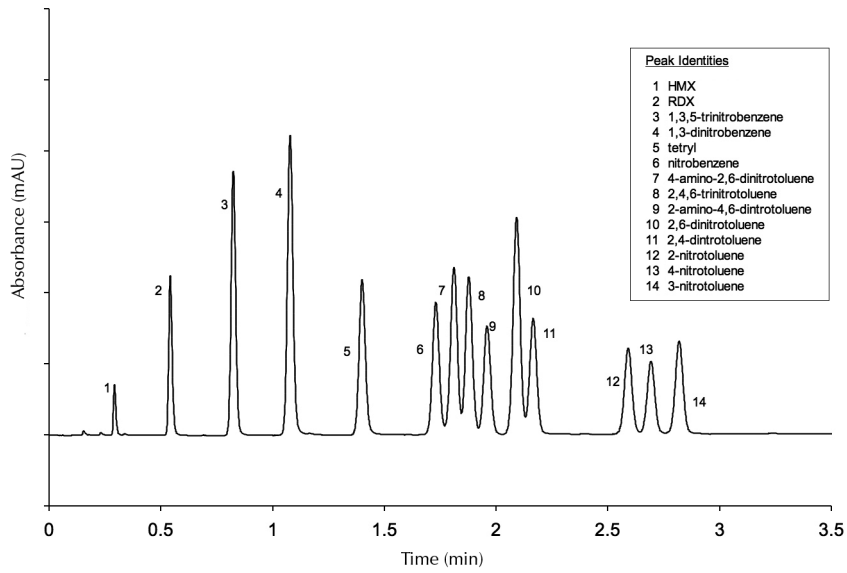

Figure 15. Rapid gradient separation of explosives. Column: 50 × 4.6 mm C18 fused-core particles; mobile phase: gradient, Solvent A = water, Solvent B = methanol, time 0.00 = 25% B, time 0.50 = 25% B, time 2.50 = 40% B; flow rate: 3.0 mL/min; temperature: 60°C; Pressure: 290 bar (initial), 325 bar (final); detection: UV at 254 nm.

pressure when measured at the plate height minimum, compared to sub-2-µm particles.

Acknowledgments

The authors thank Dr. John Salisbury of Pfizer, Inc., Dr. Mel Eureby of AstraZeneca, Professor Georges Guiochon of the University of Tennessee and W. Campbell of Supelco, Inc. for valuable data that are presented herein.

References

1. J.C. Giddings. Dynamics of Chromatography. Dekker, New York, NY, 1965, Chap. 2.
2. G.J. Kennedy and J.H. Knox. Performance of packings in high-performance liquid chromatography I. Porous and surface layered supports. *J. Chromatogr. Sci.* **10:** 549 (1972).
3. J.H. Knox. Practical aspects of LC Theory. *J. Chromatogr. Sci.* **15:** 352 (1977).
4 R.E. Majors. Anatomy of an LC column from the beginning to modern day. *LC-GC* **24:** 248–266 (2006).
5. J.W. Thompson, J.S. Mellors, J.W. Eschelbach and J.W. Jorgenson. Recent advances in ultra-high pressure liquid chromatography. *LC-GC* **24:** 16–21 (2006).
6. J.J. Kirkland. Ultra-fast reversed-phase high-performance liquid chromatographic separations: an overview. *J. Chromatogr. Sci.* **38:** 535–544 (2000).
7. J.J. Kirkland, T.J. Langlois, and J.J. DeStefano. Fused-core particles for HPLC Columns. *Am. Lab.* **39:** 18–21 (2007).
8. K. Kaczmarski and G. Giochon. Modeling of chromatographic separation using pellicular adsorbent. *Anal. Chem.* **79:** 4648–4656 (2006).
9. A. Cavazzini, F. Gritti, K. Kaczmarski, N. Marchetti, and G. Guiochon. Mass transfer kinetics in a shell material. *Anal. Chem.* **79:** 5972–5979 (2007).
10. N. Marchetti, A. Cavazzini, F. Gritti, and G. Guiochon. Gradient elution separation and peak capacity of columns packed with porous shell particles. *J. Chromatogr. A* **1163:** 203–211 (2007).
11. F. Gritti and G. Guiochon, Comparative study of the performance of columns packed with several new fine silica particles. Would the external shape of the particles affect column properties? *J. Chromatogr. A* **1166:** 30–46 (2007).
12. Y. Hsieh, C. J.G. Duncan and J.-M. Brisson. Fused-Core Silica Column High-Performance Liquid Chromatography/Tandem Mass Spectrometric Determination of Rimonabant in Mouse Plasma. *Anal. Chem.* **79:** 5668–5673 (2007).
13. L.R. Snyder and J.J. Kirkland. *Introduction to Modern Liquid Chromatography,* 2nd ed. John Wiley and Sons, New York, NY, 1979, Chapter 7.
14. J.J. Kirkland and J.J. DeStefano. The art and science of forming packed analytical high-performance liquid chromatography columns. *J. Chromatogr. A* **1126:** 50–57 (2006).
15. L.R. Snyder, J.J. Kirkland, and J.L. Glajch. *Practical HPLC Method Development,* 2nd ed. John Wiley and Sons, New York, NY, 1997, Chap. 2.
16. J. Billen, P. Gzil, F. Lynen, P. Sandra, P. van der Meeren, and G. Desmet. Poster Presentation. *HPLC 2006,* San Francisco, CA, June 2006.
17. K.K. Unger and E. Weber. *A Guide to Practical HPLC.* Git Verlag GMBH, Darmstadt, 1999, p. 45.
18. F. Gritti, A. Cavazzini, N. Marchetti, and G. Guiochon. Comparison between the efficiencies of columns packed with fully and partially porous C18-bonded silica materials. *J. Chromatogr. A* **1157:** 289–303 (2007).

Manuscript received September 7, 2007;
revision received October 5, 2007.